Differential cross sections for the electron-impact ionization of molecular hydrogen in the distorted-wave Born approximation

R. W. Zurales and R. R. Lucchese
Department of Chemistry, Texas A&M University, College Station, Texas 77843-3255
(Received 17 September 1987)

Differential cross sections for electron-impact ionization of molecular hydrogen are presented in the factorized first Born, fixed-nuclei, frozen-core Hartree-Fock approximation. The wave function of the ejected electron is described by a Coulomb wave distorted by the static-exchange potential of the frozen ionic core. Transition matrix elements are evaluated in both the length and velocity forms using Padé-approximant corrections to initial estimates based on the Schwinger variational principle. For high-energy incident electrons, the length form is in excellent agreement with experimental Compton defects but the magnitude of the doubly differential cross section is too large. The magnitude of the doubly differential cross section in the velocity form is generally in good agreement with experiment; however, the maxima occur at energy losses which are too large, particularly for small linear-momentum transfers. Results of calculations of the triply differential cross section are also presented. The agreement with experiment is only fair for 250-eV incident electrons because of the breakdown of the first Born approximation.

I. INTRODUCTION

Theoretical calculations of the differential cross section (DCS) for electron-impact ionization of molecules have generally been restricted to approximate methods which emphasize the description of the molecular bound states while essentially treating the continuum electrons as plane waves.[1] Examples of these methods are the plane-wave impulse approximation,[2,3] which has been used to compute the triply differential cross section (TDCS), and the binary-encounter approximation[4] (BEA), which has been used to compute the doubly differential cross section (DDCS). Although these plane-wave theories are generally successful when the continuum electron energies are high, the neglect of interactions with the ionized target can become significant for low ejected-electron energies. In the present paper we will consider the impact ionization of molecules in the Born approximation (BA), where only the wave functions of the relatively high-energy incident and scattered electrons are treated as plane waves. A recent calculation of the TDCS for ionization of helium, based on the factorized BA, described the wave function of the ejected electron by an orthogonalized Coulomb wave (OCW) with an empirically determined asymptotic charge.[5] This approximate treatment of distortion was capable of providing good agreement with experiment for this atomic system. However, due to the nonspherical nature of molecular systems, it may be necessary to include the effects of distortion more accurately. In the present paper we begin an investigation of the effect of distortion in molecular systems by applying the distorted-wave BA to the DCS for electron-impact ionization of molecular hydrogen.

The major difficulty in allowing for distortion in molecular systems is the calculation of multicenter-scattering wave functions. We apply a technique, developed in recent studies of molecular photoionization and low-energy electron-molecule scattering, which is based on the Schwinger variational principle and involves corrections to the initial variational estimate using $[N/N]$ Padé approximants.[6] The interaction of the ejected electron with the ionized target is approximated by the static-exchange potential evaluated in the frozen-core Hartree-Fock (FCHF) approximation. Since our initial- and final-state wave functions are solutions of a Hamiltonian with a nonlocal potential, the generalized oscillator strength (GOS) does not necessarily satisfy the Bethe sum rule and the DCS's calculated in the length and velocity forms are not equivalent. However, it has been empirically determined from photoionization studies that calculations using the velocity form are generally less sensitive to initial-state correlations.[7] In addition, although not the only source of error, the discrepancy between the length and velocity DCS's gives an estimate of the minimum error in the calculation due to the frozen-core and Hartree-Fock approximations.

A second complication for molecular systems compared to atomic systems is the treatment of nuclear motion. In the present study we apply the fixed-nuclei approximation which essentially requires the DCS to be averaged over nuclear orientations.[8] This angular averaging is performed analytically by using single-center spherical harmonic expansions of all functions. This also allows the TDCS to be expressed as a linear combination of Legendre polynomials whose coefficients are given in terms of an angular-momentum-transferred summation.[8] Although a large number of matrix elements are generally required to converge the DCS, we simplify the calculations by neglecting the relatively small distortion of higher partial waves.

For high-energy incident electrons, we find the distorted-wave velocity approximation (DWVA) to generally be in excellent agreement with experimental

DDCS's. However, particularly at small linear-momentum transfers, the calculated maximum of the DDCS occurs at too high of an energy loss. Conversely, although the distorted-wavelength approximation (DWLA) is in excellent agreement with experimental Compton defects, the calculated DDCS is too large for nearly all ejected electron energies and momentum transfers. Not surprisingly, the effects of distortion are relatively small for molecular hydrogen and similar, though less successful, results are obtained in the Coulomb-wave velocity approximation (CWVA) and the Coulomb-wavelength approximation (CWLA). We also compare our calculated TDCS's to experimental results obtained at incident energies of 250 eV. Although the agreement with experiment is only fair, the discrepancy is in large part due to the breakdown of the first Born approximation and better comparisons might be obtained at higher incident energies.

II. THEORY

The TDCS for electron-impact ionization is a measure of the probability that an incident electron of momentum $\mathbf{k}_1$ will collisionally ionize a target producing electrons of asymptotic momenta $\mathbf{k}_2$ and $\mathbf{k}_3$ which are subsequently detected in solid angles $d\Omega_2$ and $d\Omega_3$. An integral representation of the TDCS can be derived by considering the asymptotic form of $|\Psi_i\rangle$, where $|\Psi_i\rangle$ is an exact solution of the Schrödinger equation with appropriate boundary conditions. Neglecting the mass of the electrons in comparison to the mass of the nuclei, the TDCS for a spatially unpolarized system is given in atomic units by[9,10]

$$\frac{d^3\sigma}{d\Omega_2 d\Omega_3 d\epsilon}=(k_2k_3/k_1)(2\pi)^{-5}\sum_{\text{average}}|T_{fi}|^2 , \quad (1)$$

where $d\epsilon$ is an energy interval of one of the final-state continuum electrons, the summation and average refer to a summation over unresolved final states and an average over populated initial states for a given set of experimental conditions, and T_{fi} is a transition matrix element. The transition matrix element is of the form

$$T_{fi}=\langle\Psi_i|(H_t-E_t)|\Psi_f\rangle , \quad (2)$$

where H_t and E_t are the total Hamiltonian and energy of the system, respectively, and $|\Psi_f\rangle$ is a wave function which essentially describes the final state of the ionization process.[9,10]

We consider the rotationally and vibrationally unresolved TDCS in the factorized first Born fixed-nuclei approximation where the possibility of electron capture is neglected. In the BA, neglecting exchange and capture, the transition matrix element can be written as[11]

$$T_{fi}=(4\pi/K^2)\langle\psi_i|\sum_u \exp(-i\mathbf{K}\cdot\mathbf{r}_u)|\psi_f\rangle , \quad (3)$$

where $\mathbf{K}$, the linear-momentum transferred, is given by

$$\mathbf{K}=\mathbf{k}_1-\mathbf{k}_2 , \quad (4)$$

the summation runs over all target electrons, $|\psi_i\rangle$ is the initial-state target wave function, and $|\psi_f\rangle$ is the final-state target wave function. The TDCS given by Eqs. (1) and (3), evaluated in the fixed-nuclei approximation, can be expressed as[8]

$$\frac{d^3\sigma}{d\Omega_2 d\Omega_3 d\epsilon}=(k_2k_3/k_1)(4/K^4)C_{\text{ex}}(K,k_1)I(\mathbf{K},\mathbf{k}_3) , \quad (5)$$

where C_{ex} is an approximate correction for exchange scattering given by[11]

$$C_{\text{ex}}(K,k_1)=1-(K/k_1)^2+(K/k_1)^4 , \quad (6)$$

$I(\mathbf{K},\mathbf{k}_3)$ is a transition probability averaged over nuclear orientations,

$$I(\mathbf{K},\mathbf{k}_3)=(8\pi^2)^{-1}\int d\beta\sin\beta\int d\alpha\int d\gamma\,|f(\mathbf{K},\mathbf{k}_3)|^2 , \quad (7)$$

$f(\mathbf{K},\mathbf{k}_3)$ is a purely electronic transition matrix element for a fixed nuclear orientation,

$$f(\mathbf{K},\mathbf{k}_3)=(2\pi)^{-3/2}\langle\psi_f^{\text{el}}|\sum_u \exp(i\mathbf{K}\cdot\mathbf{r}_u)|\psi_i^{\text{el}}\rangle , \quad (8)$$

and $|\psi_i^{\text{el}}\rangle$ and $|\psi_f^{\text{el}}\rangle$ are the electronic wave functions of the initial and final target states, respectively. We refer to Eq. (8) as the length form of the transition matrix element. An equivalent velocity form of the purely electronic transition matrix element is given by

$$f(\mathbf{K},\mathbf{k}_3)=(2\pi)^{-3/2}(E)^{-1}\times\langle\psi_f^{\text{el}}|\sum_u[H,\exp(i\mathbf{K}\cdot\mathbf{r}_u)]|\psi_i^{\text{el}}\rangle , \quad (9)$$

where H corresponds to the electronic Hamiltonian and E is the energy loss. Equation (9) is used below to evaluate the velocity form of the TDCS.

Evaluating Eq. (8) in the FCHF approximation, the purely electronic transition matrix element in the length form is given by

$$f^L(\mathbf{K},\mathbf{k}_3)=(2\pi)^{-3/2}(\eta)^{1/2}\times\langle\psi^{\text{ej}}(\mathbf{k}_3)|(1-P)\exp(i\mathbf{K}\cdot\mathbf{r})|\psi\rangle , \quad (10)$$

where η is the occupation number of $|\psi\rangle$, the normalized Hartree-Fock orbital from which the electron is ejected, P is a projection operator given by

$$P=\sum_\alpha|\psi_\alpha\rangle\langle\psi_\alpha| , \quad (11)$$

the sum being over all occupied orbitals, and $|\psi^{\text{ej}}(\mathbf{k}_3)\rangle$ is the wave function of the ejected electron. Evaluating Eq. (9) in the FCHF approximation, the purely electronic transition matrix element in the velocity form is given by

$$f^V(\mathbf{K},\mathbf{k}_3)=(2\pi)^{-3/2}(\eta)^{1/2}(E)^{-1}\langle\psi^{ej}(\mathbf{k}_3)\,|\,(1-P)\exp(i\mathbf{K}\cdot\mathbf{r})(\tfrac{1}{2}K^2-i\mathbf{K}\cdot\nabla)\,|\,\psi\rangle\ . \tag{12}$$

In general, the matrix elements given by Eqs. (10) and (12) are not equal due to the use of the frozen-core approximation and the neglect of electron correlation.

We consider the wave function of the ejected electron to be a solution of the Lippmann-Schwinger equation,

$$(1-G^{(-)}V)\,|\,\psi^{ej}(\mathbf{k}_3)\rangle=|\,\phi(\mathbf{k}_3)\rangle\ , \tag{13}$$

where $G^{(-)}$ is a Coulomb Green's function with incoming spherical waves, V is the difference between a pure Coulombic potential and the singlet-coupled interaction potential between an electron and the frozen ionic core calculated in the static-exchange approximation, and $|\,\phi(\mathbf{k}_3)\rangle$ is a Coulomb wave satisfying the normalization condition

$$\langle\phi(\mathbf{k}_3')\,|\,\phi(\mathbf{k}_3)\rangle=(2\pi)^3\delta(\mathbf{k}_3'-\mathbf{k}_3)\ . \tag{14}$$

In view of Eq. (13), the purely electronic transition matrix element can be written as

$$f^{L,V}(\mathbf{K},\mathbf{k}_3)=U^{L,V}(\mathbf{K},\mathbf{k}_3)+D^{L,V}(\mathbf{K},\mathbf{k}_3)\ , \tag{15}$$

where the undistorted terms $U^{L,V}(\mathbf{K},\mathbf{k}_3)$ are given by

$$U^{L,V}(\mathbf{K},\mathbf{k}_3)=\langle\phi(\mathbf{k}_3)\,|\,(1-P)\exp(i\mathbf{K}\cdot\mathbf{r})\,|\,\psi^{L,V}\rangle\ , \tag{16}$$

the distortion terms $D^{L,V}(\mathbf{K},\mathbf{k}_3)$ are given by

$$D^{L,V}(\mathbf{K},\mathbf{k}_3)=\langle\psi^{ej}(\mathbf{k}_3)\,|\,V\,|\,R^{L,V}(\mathbf{K})\rangle\ , \tag{17}$$

and where

$$|\,R^{L,V}(\mathbf{K})\rangle=G^{(+)}(1-P)\exp(i\mathbf{K}\cdot\mathbf{r})\,|\,\psi^{L,V}\rangle\ , \tag{18}$$

$$|\,\psi^{L}\rangle=(2\pi)^{-3/2}(\eta)^{1/2}\,|\,\psi\rangle\ , \tag{19}$$

and

$$|\,\psi^{V}\rangle=(2\pi)^{-3/2}(\eta)^{1/2}(E)^{-1}(\tfrac{1}{2}K^2-i\mathbf{K}\cdot\nabla)\,|\,\psi\rangle\ . \tag{20}$$

If the effects of distortion are neglected, then only the first term in Eq. (15) is retained.

A consideration of the equation

$$|\,R(\mathbf{K})\rangle=(1-G^{(+)}V)\,|\,\chi(\mathbf{K})\rangle\ , \tag{21}$$

and the trial functions χ_t and ψ_t^{ej} leads to a Schwinger-type variational expression[6] for the distortion term of Eq. (15),

$$D(\mathbf{K},\mathbf{k}_3)\approx\langle\psi_t^{ej}(\mathbf{k}_3)\,|\,V\,|\,R(\mathbf{K})\rangle+\langle\phi(\mathbf{k}_3)\,|\,V\,|\,\chi_t(\mathbf{K})\rangle-\langle\psi_t^{ej}(\mathbf{k}_3)\,|\,V-VG^{(+)}V\,|\,\chi_t(\mathbf{K})\rangle\ . \tag{22}$$

We determine a zeroth-order variational estimate to $D(\mathbf{K},\mathbf{k}_3)$, D_0, by expanding the trial functions as linear combinations of basis functions and requiring that D_0 be variationally stable with respect to the expansion coefficients. We then compute a sequence of Padé approximants of the form $[N/N]$ for the error in the initial variational estimate and obtain the variational estimates D_N, which are rapidly convergent.[6] We note that if the final result is well converged, the calculation is independent of the initial basis set.

In order to evaluate the integral over Euler angles in Eq. (7) analytically, we expand the purely electronic transition matrix element in terms of spherical harmonics,

$$f(\mathbf{K},\mathbf{k}_3)=\sum_{n,j_3,J_{12}}f_{nj_3J_{12}}(K,k_3)[Y^n_{J_{12}}(\hat{\mathbf{K}})]^*Y^n_{j_3}(\hat{\mathbf{k}}_3)\ . \tag{23}$$

The TDCS given in Eq. (5) is a function of the angle between the linear-momentum transferred and the momentum of the ejected electron and can be expressed as a series in Legendre polynomials,[8]

$$\frac{d^3\sigma}{d\Omega_2\,d\Omega_3\,d\epsilon}=(k_2k_3/k_1)(4/K^4)C_{ex}(K,k_1)\times(4\pi)^{-1}\sum_l a_l(K,k_3)P_l(\cos\theta)\ . \tag{24}$$

The expansion coefficients a_l, expressed as a summation in terms of J, the angular-momentum transferred, are given by[8]

$$a_l(K,k_3)=(4\pi)^{-1}\sum_J\sum_{j_3,J_{12}}\sum_{j_3',J_{12}'}[(2J_{12}+1)(2j_3+1)(2J_{12}'+1)(2j_3'+1)]^{1/2}(-1)^{J+l}\langle j_30j_3'0\,|\,l0\rangle\langle J_{12}0J_{12}'0\,|\,l0\rangle\times\begin{Bmatrix}j_3 & j_3' & l\\ J_{12}' & J_{12} & J\end{Bmatrix}F_{Jj_3J_{12}}(K,k_3)[F_{Jj_3'J_{12}'}(K,k_3)]^*\ , \tag{25}$$

where $\langle jmj'm'\,|\,JM\rangle$ is a Clebsch-Gordan coefficient, the quantity in curly brackets is a Wigner 6-j coefficient, and the angular-momentum-transferred transition matrix elements are given by[8]

$$F_{Jj_3J_{12}}(K,k_3)=\sum_n(-1)^n\langle J_{12}-nj_3n\,|\,J0\rangle\times f_{nj_3J_{12}}(K,k_3)\ . \tag{26}$$

In general, a large number of matrix elements are required to converge the TDCS. For high angular momenta, however, the effects of distortion are relatively unimportant. Therefore, for values of j_3 greater than some maximum value j_D we neglect the effects of distortion. This greatly simplifies the expression for, and the calculation of, the transition matrix elements.

Integrating Eq. (24) over the directions of the ejected electron, we obtain a DDCS which is given by[8]

$$\frac{d^2\sigma}{d\Omega_2 d\epsilon}=(k_2k_3/k_1)(4/K^4)C_{\rm ex}(K,k_1)a_0(K,k_3)\ , \quad (27)$$

where, from Eq. (15), the coefficient $a_0(K,k_0)$ can be written as

$$a_0(K,k_3)=(4\pi)^{-1}\sum_{J,j_3,J_{12}}|F_{Jj_3J_{12}}(K,k_3)|^2\ . \quad (28)$$

We note that the DDCS given in Eq. (27) corresponds to the cross section for the production of a given final state of the ionized target.

A DDCS may also be defined where only the energy lost by the incident electron is known and no knowledge of the energy of the ejected electron is assumed. This cross section is obtained by summing the cross section of Eq. (27) over all possible final target states for the given energy loss. In the factorized BA, the cross-section differential with respect to the solid angle of the scattered electron and the energy loss can be written as[11]

$$\frac{d^2\sigma}{d\Omega_2 dE}=(k_2/k_1)(4/K^4)(K^2/E)C_{\rm ex}(K,k_1)\frac{df(K,E)}{dE}\ , \quad (29)$$

where the GOS is defined as

$$\frac{df(K,E)}{dE}=[E/(8\pi^3K^2)]\times\sum_{\rm average}\left|\left\langle\psi_f\left|\sum_u\exp(i\mathbf{K}\cdot\mathbf{r}_u)\right|\psi_i\right\rangle\right|^2\times\delta(E+E_i-E_f)\ , \quad (30)$$

E_i is the energy of the initial target state and E_f is the energy of the final target state. The partial GOS for the production of a given final target state can be obtained by comparing Eq. (29) with Eq. (27) and is given by

$$\frac{df(K,E)}{dE}=(Ek_3/K^2)a_0(K,k_3)\ , \quad (31)$$

where the momentum of the ejected electron is obtained from

$$\tfrac{1}{2}k_3^2=E-V_{\rm IP}\ , \quad (32)$$

and $V_{\rm IP}$ is the ionization potential. In the limit of small linear-momentum transfers, the GOS is equal to the dipole optical oscillator strength and we obtain an approximation to the total photoionization cross section given by[6,7]

$$\sigma_P(E)=(4\pi^2/3c)\lim_{K\to0}(Ek_3/K^2)a_0(K,k_3)\ , \quad (33)$$

where c is the speed of light.

Another related quantity is the Compton profile, defined by[11]

$$J(q,K)=(K^3/E)\frac{df(K,E)}{dE}\ , \quad (34)$$

where

$$q=(E-\tfrac{1}{2}K^2)/K\ . \quad (35)$$

The Compton profile is given in our approximation by

$$J(q,K)=(Kk_3)a_0(K,k_3)\ , \quad (36)$$

whereas in the BEA, the Compton profile is given by[11]

$$J(q)=2\pi\int_{|q|}^{\infty}dp\,p\rho(p)\ , \quad (37)$$

where $\rho(p)$ is the spherically averaged molecular momentum density. We note that in the BEA, the peak height of the Compton profile is independent of K and the location of the peak is at $q=0$.

At incident energies sufficiently high for the BA to be valid, relativistic effects may become important. Therefore, at high incident-electron energies, we use relativistic energies and momenta and we include in the definition of our approximate DDCS, Eq. (27), the multiplicative relativistic correction factor $C_{\rm rel}$ given by[4]

$$C_{\rm rel}=\frac{1-(E/c^2)(1-\beta^2)^{1/2}}{[1-(E/cK)^2]^2(1-\beta^2)}\ , \quad (38)$$

where β is the ratio of the incident electron velocity to c. In addition, we include the relativistic corrections to $C_{\rm ex}$ suggested by Bonham and Tavard[4] and note that the relativistic BEA definition of q is given by[4]

$$q=[E+(E^2/2c^2)-\tfrac{1}{2}K^2]/K\ . \quad (39)$$

III. METHOD

The initial-state wave function for H_2 which we use in our calculations is the restricted-Hartree-Fock wave function of Cade and Wahl[12] which was constructed from 12 Slater-type orbitals centered at each nucleus with an equilibrium nuclear separation of 1.4 a.u. In all calculations, we assume that only the ground state of H_2^+ is produced in the ionization and that the ionization potential for producing H_2^+ in the ground state is 16.4 eV, which is the vertical ionization potential.[13]

The initial basis set for the trial wave functions for the scattering calculations is similar to the set used in a recent study of the photoionization of H_2.[14] For each symmetry, the initial basis set consists of four spherical Gaussians centered at each nucleus and one spherical Gaussian centered at the bond midpoint. With this choice of initial basis set, the $[N/N]$ Padé approximants for the matrix elements are converged with $N=1$.

To evaluate all matrix elements needed to compute the Padé approximants, we re-expand the target and trial wave functions about the bond midpoint in a linear combination of, at most, 12 products of radial functions and spherical harmonics of the appropriate symmetry. In evaluating the static-exchange potential, all resulting direct and exchange integrals are computed without further truncation in the spherical harmonics. A maximum of 60 partial waves are used in the expansions of Coulomb-wave and plane-wave functions, but J of Eq. (25) is restricted to a maximum of 6. The maximum

value of j_D is 12, and all possible symmetries consistent with j_3 are included in the evaluation of the angular-momentum transferred transition matrix elements. For each K and k_3, the parameters were chosen so as to converge the DDCS to four significant figures.

All radial integrals are computed using numerical quadrature as is described elsewhere.[15] The integrals are evaluated on a grid of 970 points extending out to 32.0 a.u. The smallest grid spacing of 0.005 a.u. is used for points within 0.3 a.u. of the nuclei. The largest grid spacing is 0.04 a.u.

IV. RESULTS

For incident energies in excess of 20 keV, the results of several experiments have suggested that the first Born approximation, with the inclusion of corrections for relativistic and exchange effects, is valid for the determination of the GOS.[16–18] In the BEA, the GOS is obtained from Eqs. (34) and (37). As part of an investigation to determine the validity of the BEA, Rueckner, Barlas, and Wellenstein performed experiments on molecular hydrogen which accurately measured the location of the maximum of the Compton profile as a function of the linear-momentum transferred.[18] The experimental evidence indicates that even at comparatively large linear-momentum transfers, the BEA breaks down in the high accuracy limit. The BEA is based, in part, on the assumption that the wave function of the ejected electron is accurately described by a plane wave. We have found that a more realistic treatment of the interaction of the ejected electron with the ionized target is capable of greatly improving the comparison between theory and experiment for molecular hydrogen.

The BEA predicts that the maximum in the Compton profile occurs at an energy loss E_{max} obtained by setting q equal to zero in Eq. (39). The difference between the experimental value of E_{max} and the BEA value of E_{max} has been termed the Compton defect. Using a parabolic fit of values of the Compton profile calculated in the vicinity of the maximum, we have explicitly determined the value of E_{max} for each of our approximations, DWLA, DWVA, CWLA, and CWVA. In Fig. 1 we plot the corresponding quantity q_{max} as a function of the linear-momentum transferred. The agreement between the DWLA and experimental Compton defects is excellent. The agreement between the distorted-wave calculations is good for large values of the linear-momentum transferred, but the DWVA value of E_{max} is too large at small values of K. A similar trend is found in the OCW calculations with the CWLA yielding slightly better agreement with experiment. However, although superior to the BEA, the value of E_{max} predicted by the OCW calculations is too large even for relatively high K. These results suggest that the determination of the Compton defect may be more sensitive to the description of the ejected electron than the description of the bound state.

In Fig. 2 we plot our calculated values of the peak height of the Compton profile as a function of K and include the results of BEA calculations using a self-consistent-field (SCF) target, a target wave function including configuration interaction (CI), and a vibrationally averaged CI (VACI) calculation.[19] We also include the experimental data of Lee.[20] In the BEA, the peak height is independent of the linear-momentum transferred, an approximation which becomes worse with decreasing K. Although the DWLA was the most successful in determining the location of the Compton profile peak, the DWLA is the least successful of our approximations in predicting the magnitude of the peak. The best overall agreement with experiment is obtained with the DWVA, while the CWLA overestimates the peak height and the CWVA tends to underestimate the peak height. This result is similar to photoionization studies of N_2 in which the DWVA was both in better agreement with experiment and less sensitive to initial-state correlations than the DWLA.[7]

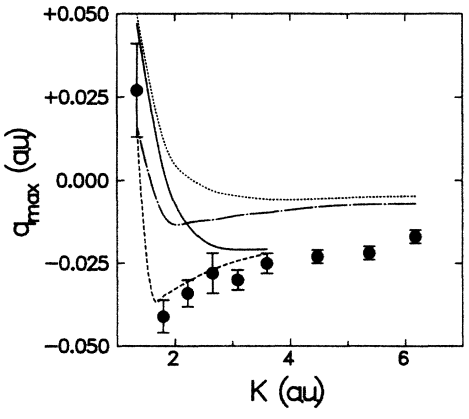

FIG. 1. Compton defect for an incident energy of 25 keV: ——, DWVA; — — —, DWLA; - - - -, CWVA; —— — ——, CWLA; solid circles, experimental results of Rueckner *et al.* (Ref. 18).

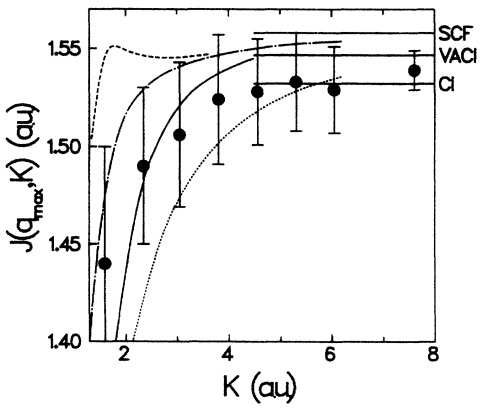

FIG. 2. Peak height of the Compton profile for an incident energy of 25 keV: —— DWVA; — — —, DWLA; - - - -, CWVA; —— — ——, CWLA; solid circles, experimental results of Lee (Ref. 20).

We next discuss the large-K convergence of the peak heights in the length form. The effect of distortion on the peak height rapidly becomes small in the length form, the DWLA and the CWLA apparently differing by less than 0.1% for linear-momentum transfers in excess of 4 a.u. While not included in Fig. 2, we have also determined the peak height of the Compton profile in the length form by describing the wave function of the ejected electron by an orthogonalized plane wave (OPW). For linear-momentum transfers in excess of 6 a.u., the use of an OPW yields results essentially indistinguishable from the BEA SCF limit. Even for K as low as 3 a.u., the correction remains small (less than 0.5%). These results indicate that the BEA is valid for the determination of the peak height at large K and that the peak height of the Compton profile is a sensitive test of the description of the molecular target state.

In contrast to the length form, calculations in the velocity form are sensitive to the description of the ejected electron and the convergence of the peak heights is comparatively slow. Although the difference between the DWLA and the DWVA is small (less than 0.3%) for K greater than 4 a.u., the CWLA and CWVA still differ by more than 1.0% for values of K as large as 6 a.u. In addition, the use of an OPW predicts the peak height to be much smaller in the velocity form than in the length form, nearly 9.0% smaller at linear-momentum transfers as large as 6 a.u.

In an attempt to understand the discrepancy between calculations in the length and velocity form, reconsider the equivalent length and velocity forms of the matrix element

$$M_L = \langle \Psi_f \mid \exp(i\mathbf{K}\cdot\mathbf{r}) \mid \Psi_i \rangle \ , \tag{40a}$$

$$M_V = \langle \Psi_f \mid [H, \exp(i\mathbf{K}\cdot\mathbf{r})] \mid \Psi_i \rangle / E \ , \tag{40b}$$

where Ψ_i and Ψ_f are the exact wave functions for the initial and final target states. In the BA, matrix elements arise which are of the form of Eq. (40) but with an additional term which is introduced to enforce orthogonality between the initial and final target states. Although this additional term is zero for the exact wave functions, it is not necessarily zero for approximate wave functions. The required matrix element in the length form for approximate wave functions can be written as

$$M_L = \langle \psi_f \mid \exp(i\mathbf{K}\cdot\mathbf{r}) \mid \psi_i \rangle - \langle \psi_f \mid \psi_i \rangle \langle \psi_i \mid \exp(i\mathbf{K}\cdot\mathbf{r}) \mid \psi_i \rangle \ , \tag{41}$$

where the second term ensures the orthogonality of the approximate states. As long as the initial-state wave function is a real function, this additional term does not appear in the velocity form. Therefore, the matrix element in the velocity form for approximate wave functions may be expanded as

$$M_V = \langle \psi_f \mid \exp(i\mathbf{K}\cdot\mathbf{r}) \mid \psi_i \rangle + \langle \psi_f \mid (V_f/E)\exp(i\mathbf{K}\cdot\mathbf{r}) - \exp(i\mathbf{K}\cdot\mathbf{r})(V_i/E) \mid \psi_i \rangle \ , \tag{42}$$

where V_f (V_i) is the part of the potential which is not included in the Hamiltonian of the approximate final-state (initial-state) wave function. The length form essentially involves a correction term based on the overlap of the approximate wave functions, while the velocity form essentially involves corrections based on the neglected potentials.

If the integral containing the neglected potential is small compared to the energy loss and the overlap is negligible, the length and velocity forms will yield equivalent numerical values. Not surprisingly, the results of calculations using an OPW in the length form indicated that the effects of orthogonalization are relatively small for large ejected-electron energies. Therefore, the matrix element in the length form is well approximated by the first term of Eq. (41) at high energies. This suggests that the rate of convergence of the length and velocity forms for a particular choice of ejected electron wave function is indicative of the magnitude of the neglected potential. Apparently, even at high linear-momentum transfers, the magnitude of the neglected potential is relatively large when the ejected-electron wave function is treated as a plane wave. We conclude that although the BEA accurately describes the peak height of the Compton profile, the poor description of the interaction of the ejected electron with the ionized target is responsible for the large discrepancy between the length and velocity forms as well as the Compton defect. Furthermore, even the Coulomb wave calculations appear to be inadequate in the high accuracy limit, and only the distorted-wave calculations yield good agreement with experimental Compton defects.

Thus far, we have concentrated on the location and magnitude of the peak of the Compton profile as a function of K. We next discuss the DDCS as a function of the energy loss. In Fig. 3 we plot the high-E portion of

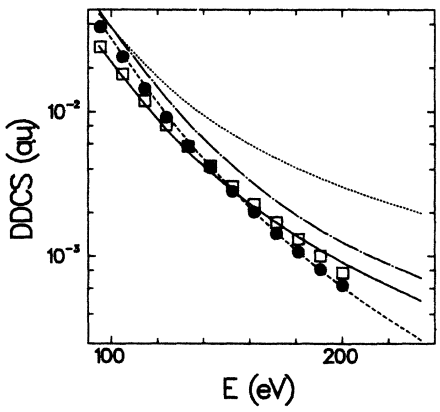

FIG. 3. Doubly differential cross section for an incident energy of 25 keV. For $K=0.7953$ a.u.: ——, velocity approximation; - - - -, length approximation; open squares, experiment. For $K=1.552$ a.u.: — — —, velocity approximation; ——— — ———, length approximation; solid circles, experiment. Experimental data are representative points from the experimental curve of Ulsh *et al.* (Ref. 17).

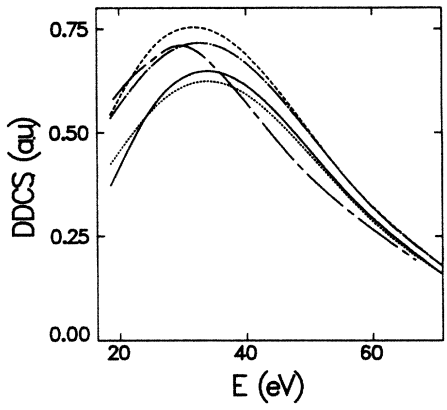

FIG. 4. Doubly differential cross section for an incident energy of 25 keV and linear momentum transfer of 1.552 a.u.: ——, DWVA; — — —, DWLA; - - - -, CWVA; ——-——, CWLA; —— — ——, experimental results of Ulsh *et al.* (Ref. 17).

the DDCS for an incident energy of 25 keV and linear-momentum transfers of 0.7953 and 1.552 a.u. and include the experimental data of Ulsh, Wellenstein, and Bonham.[17] At large ejected-electron energies, the effect of distortion is relatively small and the distorted-wave and OCW calculations are essentially indistinguishable on the scale of Fig. 3. Although the DDCS calculated in the length form is too large, the agreement with experiment is excellent for calculations in the velocity form. The good agreement in the velocity form is probably due to the approximate inclusion of initial-state correlations and the comparatively small effects of final-state correlations for high-energy ejected electrons.

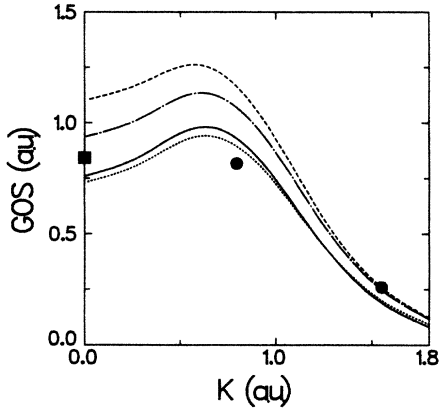

FIG. 5. Generalized oscillator strength for ejected-electron energy of 4.5 eV: ——, DWVA; — — —, DWLA; - - - -, CWVA; —— — ——, CWLA; solid circles, experimental results of Ulsh *et al.* (Ref. 17); solid square, interpolated from the experimental results of Samson and Cairns (Ref. 23) and the experimental results of Cook and Metzger (Ref. 24).

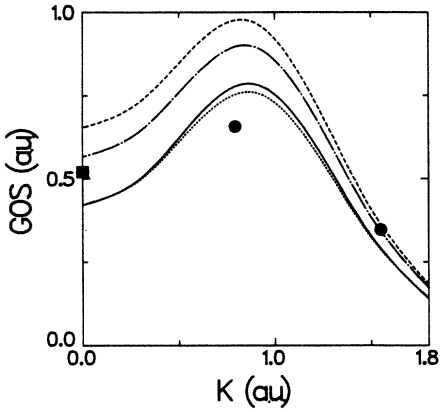

FIG. 6. Generalized oscillator strength for an ejected-electron energy of 9.0 eV (same designations as in Fig. 5).

In Fig. 4 we plot the low-energy portion of the DDCS for a K of 1.552 a.u. Although excellent agreement was obtained with experiment at high E, the DDCS in the velocity form is too small at low E and slightly too large at moderate E. For E less than 30 eV, calculations in the length form are actually in better agreement with experiment than those in the velocity form. The agreement with experiment might be improved by explicitly including initial-state correlations. Although the velocity form approximately includes initial-state correlations, the correction has generally been found to increase with decreasing E,[7] as suggested by Eq. (42). This may also explain the low-K disagreement between the calculated Compton defect in the length and velocity forms. However, particularly at low ejected-electron energies, final-state correlations may be significant.

We have also calculated values of the GOS as a function of K for ejected-electron energies of 4.5 eV (Fig. 5) and 9.0 eV (Fig. 6). Even at these relatively low ejected-

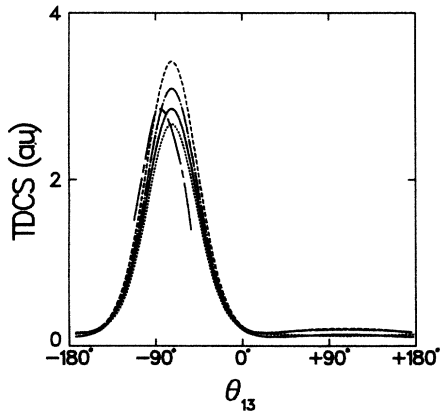

FIG. 7. Triply differential cross section for an incident energy of 250 eV, an ejected electron energy of 4.5 eV, and $\theta_{12}=12°$: ——, DWVA; — — —, DWLA; -----, CWVA; —— — ——, CWLA; —— — ——, experimental results of Jung *et al.* (Ref. 21). The binary peak of the experimental results has been normalized to the binary peak in the DWVA.

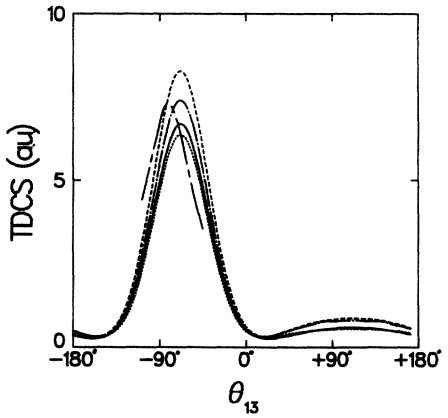

FIG. 8. Triply differential cross section for an incident energy of 250 eV, an ejected-electron energy of 4.5 eV, and $\theta_{12}=8°$ (same designations as in Fig. 7).

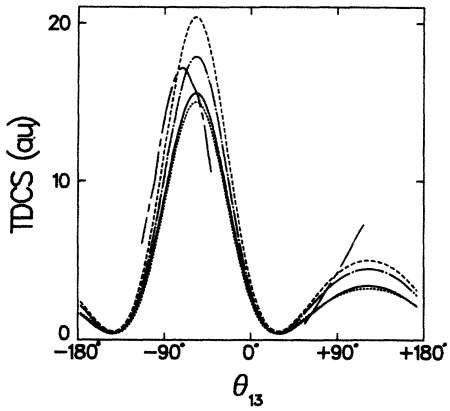

FIG. 9. Triply differential cross section for an incident energy of 250 eV, an ejected-electron energy of 4.5 eV, and $\theta_{12}=4°$ (same designations as in Fig. 7).

electron energies, the use of an OCW provides a good approximation to the effects of distortion, particularly in the velocity form. In general, the difference between the distorted-wave and OCW results is smaller than the difference between the length and velocity results. This suggests that the discrepancy in the length and velocity calculations may in large part be due to initial-state correlations.

The previous comparisons between theory and experiment have been based on data obtained at incident energies sufficiently high for the first Born approximation to be valid. We next compare our results to the experimental TDCS's measured by Jung *et al.* at an incident energy of 250 eV and an ejected-electron energy of 4.5 eV.[21] Since the experimental cross sections are only relative, we have arbitrarily normalized the binary peak of the experimental cross section for $\theta_{12}=12°$ to the binary peak in the DWVA (Fig. 7). We present our results for $\theta_{12}=8°$ in Fig. 8 and for $\theta_{12}=4°$ in Fig. 9. The most obvious discrepancy between theory and experiment is in the location of the binary peak. This discrepancy indicates the breakdown of the factorized first Born approximation. Nevertheless, the relative magnitudes of the binary peaks are in fair agreement with experiment. However, as Fig. 9 indicates, the magnitude of the recoil peak is greatly underestimated in the first Born approximation. These results are similar to those obtained in studies of atomic systems at low incident energies.[22] Better agreement with experiment might be obtained at higher incident energies, as suggested by a recent study of helium.[5]

V. CONCLUSION

The explicit inclusion of distortion has a relatively minor effect on the DCS for electron-impact ionization of molecular hydrogen and the description of the ejected-electron by an OCW is generally a good approximation. However, an accurate treatment of the interaction between the ejected-electron and the ionized target is important in the determination of the Compton defect. Calculations in the velocity form are generally in better agreement with experiment than calculations in the length form. This may be due to the approximate inclusion of initial-state correlations in the velocity form. However, further improvement might be obtained by using an explicitly correlated initial-state wave function.

Although a relatively minor effect in H_2, distortion may be more important for larger molecular systems. We are currently performing calculations of the DCS for electron-impact ionization of N_2. Although the discrepancy between the length and velocity DCS's gives an estimate of the error in the calculation, the nonequivalence makes comparisons with experiment more difficult. We are presently investigating the possibility of calculating the GOS in the random-phase approximation. In this approximation, the length and velocity forms would be equivalent and the GOS would satisfy the Bethe sum rule.

ACKNOWLEDGMENTS

Acknowledgment is made to the Monsanto Company, to the Dow Chemical Company Foundation, and to the Celanese Chemical Company for partial support of this research. In addition, this material is based upon work in part supported by the National Science Foundation under Grant No. CHE-83-51414 and in part supported by the Robert A. Welch Foundation (Houston, TX) under Grant No. A-1020.

[1]See, for example, *Electron Impact Ionization*, edited by T. D. Mark and G. H. Dunn (Springer-Verlag, Vienna, 1985).
[2]E. Weigold and I. E. McCarthy, Adv. At. Mol. Phys. **14**, 127 (1978).
[3]I. E. McCarthy and E. Weigold, Phys. Rep. **27C**, 275 (1976).
[4]R. A. Bonham and C. Tavard, J. Chem. Phys. **59**, 4691 (1973).
[5]A. Lahmam-Bennani, H. F. Wellenstein, C. Dal Cappello, and A. Duguet, J. Phys. B **17**, 3159 (1984).

[6]R. R. Lucchese and V. McKoy, Phys. Rev. A **28**, 1382 (1983).
[7]R. R. Lucchese, G. Raseev, and V. McKoy, Phys. Rev. A **25**, 2572 (1982).
[8]R. W. Zurales and R. R. Lucchese, Phys. Rev. A **35**, 2852 (1987).
[9]M. R. H. Rudge, Rev. Mod. Phys. **40**, 564 (1968).
[10]R. K. Peterkop, *Theory of Ionization of Atoms by Electron Impact* (Colorado Associated University Press, Boulder, CO 1977).
[11]See, for example, R. A. Bonham and H. F. Wellenstein, in *Compton Scattering*, edited by B. Williams (McGraw-Hill, London, 1977), p. 234.
[12]P. E. Cade and A. C. Wahl, At. Data **13**, 339 (1974).
[13]P. H. S. Martin, T. N. Rescigno, V. McKoy, and W. H. Henneker, Chem. Phys. Lett. **29**, 496 (1974).
[14]R. R. Lucchese and V. McKoy, Phys. Rev. A **24**, 770 (1981).
[15]R. R. Lucchese, K. Takatsuka, and V. McKoy, Phys. Rep. **131**, 147 (1986).
[16]H. F. Wellenstein, R. A. Bonham, and R. C. Ulsh, Phys. Rev. A **7**, 1568 (1973).
[17]R. C. Ulsh, H. F. Wellenstein, and R. A. Bonham, J. Chem. Phys. **60**, 103 (1974).
[18]W. H. E. Rueckner, A. D. Barlas, and H. F. Wellenstein, Phys. Rev. A **18**, 895 (1978).
[19]See B. Jeziorski and K. Szalewicż, Phys. Rev. A **19**, 2360 (1979) and references within.
[20]J. S. Lee, J. Chem. Phys. **66**, 4906 (1977).
[21]K. Jung, E. Schubert, D. A. L. Paul, and H. Ehrhardt, J. Phys. B **8**, 1330 (1975).
[22]See, for example, F. W. Byron, Jr., C. J. Joachain, and B. Piraux, J. Phys. B **18**, 3203 (1985).
[23]J. A. R. Samson and R. B. Cairns, J. Opt. Soc. Am. **55**, 1035 (1965).
[24]G. R. Cook and P. H. Metzger, J. Opt. Soc. Am. **54**, 968 (1964).